Experiments and analyses of fracture properties of grouting mortars

S. Ishiguro
Graduate School of Bioresources, Mie University, Tsu, Japan

ABSTRACT: Material experiments for the grouting mortar are performed to evaluate the fracture properties. The fracture mechanical parameters such as the specific fracture energy and the tension softening diagram are analyzed from the load-displacement curves measured using rectangular notched specimens and wedge-splitting procedures. Using these data, the tension-softening diagram of the grouting mortar is proposed and applied to numerical analyses of the wedge-splitting test specimens to investigate the applicability of the model. The analytical results are compared with the experimental results, and the reliability of the tension -softening diagram is examined. It is concluded that the tension-softening diagram proposed is useful for the fracture analysis of the mortar.

1 INTRODUCTION

In this study, material experiments are conducted to evaluate the fracture properties of grouting mortar used for the repair or renewal works. Fracture parameters of the materials as well as the strengths are very important for the analyses and examination of the mechanical behaviors of renewed structures. Therefore, the experiments and analyses are focused on the evaluation of fracture properties of the grouting cement mortars, which are newly developed for the SPR (Spirally Pipe Renewal) methods.

Fracture mechanical parameters such as the specific fracture energy and the tension-softening diagram are analyzed from the load-displacement curves measured by rectangular notched specimens and wedge-splitting procedures. Using these data, a tension-softening diagram is proposed for the grouting mortar. Numerical fracture analyses of the wedge-splitting test under stable crack growth conditions are carried out to investigate the applicability of the softening models. The numerical results are compared with the experimental results, and the reliability of the tension-softening diagrams is examined and discussed.

2 MATERIAL EXPERIMENTS

2.1 Basic properties of materials

Three kinds of cement mortar (M1, M2 and M3) with siliceous sand and dried sand were tested. The mix ratio, compressive, tensile and bending strengths, are listed in Table 1 for M1, M2 and M3 mortar. In the mixtures ordinary portland cement and polyacrylic acid ester emulsion are used as a binder.

The specimens were allowed to harden for 24 hours after casting, before being removed from their molds. After the removal from the molds, the specimens were wrapped in a thin plastic sheet and stored in a chamber at a temperature of 23 ℃ until testing.

The mortar specimens were tested under the different ages of 7 and 28 days. All tests were performed on three identical specimens of each material to obtain sufficient data for a statistical evaluation. The bending strength f_b and compressive strength f_c are obtained from the tests using a bending specimen of $40mm \times 40mm \times 160mm$. The tensile strength f_t is determined from the cylindrical specimen with 75 mm height and 50 mm diameter.

2.2 Fracture testing method

A schematic of the wedge-splitting test method, originally developed by Tschegg et al. (1991, 1995), is given in Figure 1. The single-edge notched specimen is placed on a narrow linear support in a compression-testing machine. A wedge-splitting apparatus, comprised of a wedge and load transmission pieces, is placed into a groove (see Figure 1(a)). The wedge, starter notch, and linear support are vertically aligned, which allows the load to be transmitted directly from the testing machine to the specimen without producing additional lateral loads or moments.

The wedge transmits a force (F_m) from the testing machine to the specimen. This force is transformed by

the slender wedge into a large horizontal component (F_h) and a small vertical component (F_v), which are then applied to the specimen (see Figure 1(b)). The large horizontal component splits the specimen in a manner similar to a bending test. A load cell in the testing machine measures the total force (F_m). Since the wedge angle (α) is known, the horizontal component (F_h) is calculated as follows.

$$F_h = \frac{F_m}{2\tan(\alpha/2)} \qquad (1)$$

The displacement of the specimen, referred to as the Crack Mouth Opening Displacement (CMOD), is measured at each end of the groove using a clip gauge. The mean values of the two measurements (d_1 and d_2) are used to reduce the uncertainty. Tests were performed using a mechanical compression-testing machine with a load capacity of 9.8 kN. The crosshead velocity for each test was 0.67 mm/min.

A rectangular notched specimen, illustrated in Figure 2, was used for fracture tests of the mortar. A starter notch (2 mm wide) was cut in the top of the specimen with a stone saw shortly before testing. The ligament length is 60 mm for all specimens.

2.3 *Load-displacement diagram*

The force (F_m) and the two end displacements (d_1 and d_2) were recorded by an electronic data logger at 1.0-second intervals. The data were then analyzed to produce a load-displacement curve (F_h-CMOD curve).

The measured load-displacement curves are given in Figures 3 (a)~(f) for the M1, M2 and M3 mortar at the different ages. The load-displacement graphs represent the curves of the three identical specimens at each material age. The scattering of the measured data in the three specimens at each age was small in these mortar specimens. Large differences between the M1 and M3 mortar were observed in the maximum load as plotted in Figures 3(a) and (e). The results also showed that the maximum load increased slightly with the increasing material age.

3 ANALYSIS OF FRACTURE PARAMETER

The load-displacement curves indicated in Figures 3 (a)~(f) characterize the fracture properties of the mortar. In this study, the fracture mechanical parameters, such as the specific fracture energy (G_f) and the tension-softening diagram, are derived from the experimental results.

3.1 *Specific fracture energy*

The area under the load-displacement curve represents the energy needed to fracture the specimen (fracture energy). The specific fracture energy (G_f) is a measure of the crack growth resistance of the

Table 1. Properties of grouting mortar

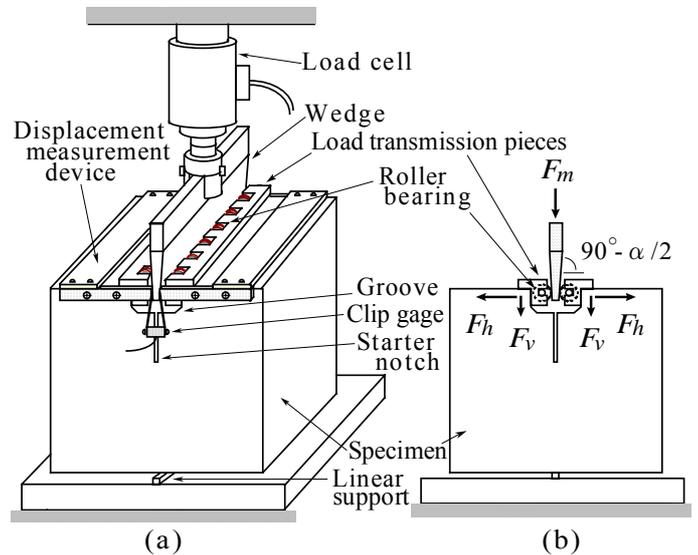|		M1	M2	M3
W/C (%)		34	40	55
P/C (%)		6.9	-	3.8
Type of aggregate		Siliceous sand	Dried sand	Siliceous sand
Type of polymeric admixture		PAE	-	PAE
Unit weight (g/cm³)		2.07	2.17	1.88
f_c (MPa)	Age (day) 7	47.7	45.1	29.1
	28	52.3	53.0	32.5
f_t (MPa)	7	3.82	2.80	2.13
	28	4.60	4.04	2.66
f_b (MPa)	7	9.86	9.06	5.99
	28	11.3	10.4	5.86

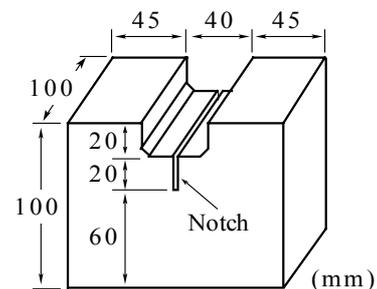Figure 1. Testing arrangement for wedge-splitting method

Figure 2. Dimensions of specimens

material and is defined as the ratio of fracture energy to fracture area, normal to the wedge penetration direction.

The specific fracture energy (G_f) of the mortar specimens is determined from the test results and is given in Figure 4. The G_f values of the M1 mortar are 0.035 and 0.038 N/mm at the age of 7 and 28 days respectively and are almost same as those of the M2 and M3 mortar (0.034~0.04 N/mm). The results also
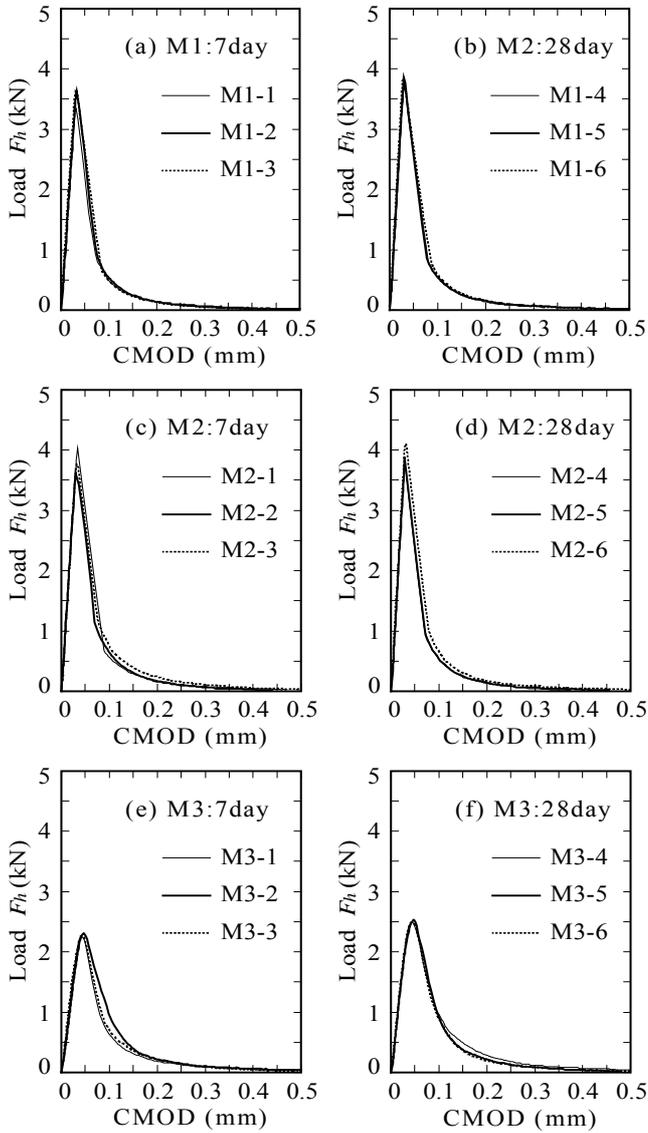
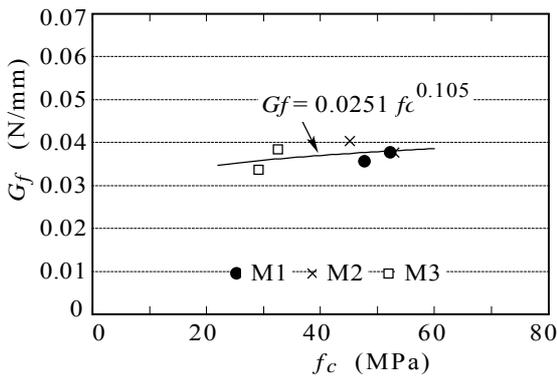Figure 3. Measured load (F_h)-displacement (CMOD) curves for mortars at different ages

Figure 4. Relationship between specific fracture energy G_f and compressive strength f_c

show that the G_f values increased slightly with the increasing compressive strength f_c as plotted in Figure 4.

The G_f value of the mortar is smaller than that obtained from the normal concrete with the same compressive strength as the mortar. This means that the crack growth resistance of the mortar is much

smaller than that of the normal concrete. The low G_f value in the mortar probably results from the lower aggregate interlock during crack propagation in comparison with the normal concrete. This may lead to a brittle failure in mortar specimens, because of the low fracture energy and the low crack growth resistance.

This result was proved by fractographic observations, which showed that the fracture surfaces of mortar specimens were flatter and less tortuous than those of concrete specimens (see Figures 5(a)~(c)).
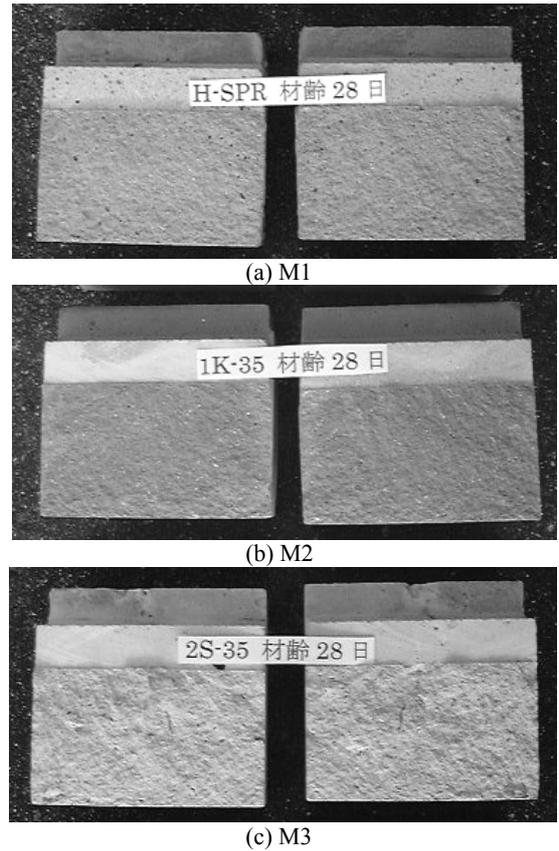

(a) M1

(b) M2

(c) M3

Figure 5. Fracture surfaces of mortar specimens

3.2 *Tension-softening diagram*

In order to characterize the fracture behavior of mortar, the strain softening behavior must be determined from a tension-softening diagram. The tension-softening diagram characterizes the relation between the crack width and the tensile stress of the materials and is useful for evaluating the toughness of new materials and fiber-reinforced concrete. The evaluation methods of the tension-softening diagram are classified into some groups (Mihashi et al. 2001). In this study, a poly-linear inverse analysis was used to determine the exact shape of the tension-softening diagram from the measured load-displacement curves.

The poly-linear inverse analysis was based on the finite element method applied using the fictitious crack model (Uchida et al. 1995), and was developed specifically for the wedge-splitting loading

conditions (Ishiguro, 2001, Ishiguro et al., 2004). Details for the inverse analysis method may be found in (Kitsutaka et al. 2001).

The characteristic values of the poly-linear softening diagram are obtained using an iterative best-fit procedure to match the calculated and measured load (F_h)-displacement (CMOD) curves. A F_{hcal}/F_{hmeas} ratio between 0.999 and 1.001 ($\pm 0.1\%$) was used as the tolerance for the fitting procedure to provide the required tension-softening diagrams from the wedge-splitting test results.

The determined tension-softening diagrams of the M1, M2 and M3 mortar are given in Figures 6 (a)~(f) for the different ages of 7 and 28 days. The results show that the computed critical crack width (W_c) is approximately 0.03 mm for the M1 and M2 mortar and 0.04 mm for the M3 mortar. The values are far smaller than that of the normal concrete (more than 0.15 mm). This shows that the mortars have the lower aggregate interlock during crack propagation. The diagrams also show that the cohesive stress of the M1 and M2 mortar is higher than that of the M3 mortar. The higher cohesive stresses in the softening curves of the M1 and M2 are induced as a result of mix proportions of the mortar.

Young's modulus (E_c) and tensile strengths (S_0) determined by the inverse analyses are listed in Table 2. The results indicate that the E_c value for the M3 mortar is almost half of that of the M1 and M2 mortar. The tensile strength (S_0) for the mortar at each age, as calculated using the iterative best-fit procedure, were larger than the measured splitting tensile strength (f_t). Figure 7 shows the relationship between the tensile strength (S_0) and the splitting tensile strength (f_t). According to the regression analysis of the data, a linear equation ($S_0 = 1.71 f_t$) is obtained.

From the analytical results coefficients β ($= W_c S_0 / G_f$) are calculated for each mortar. Figure 8 shows the relationship between the coefficient β and the compressive strength f_c. The average value of coefficients β is 4.7 for the mortar. Using these data, the critical crack width W_c is given by $W_c = 4.7 G_f / S_0$.

Table 2. Young's modulus (E_c) and tensile strength (S_0) determined by inverse analysis

	Age (day)	M1	M2	M3
E_c (GPa)	7	22.0	22.4	11.6
	28	24.4	24.6	13.0
S_0 (MPa)	7	6.13	6.77	3.51
	28	6.95	7.43	3.94

4 FRACTURE ANALYSIS OF MORTAR

4.1 *Tensile softening model*

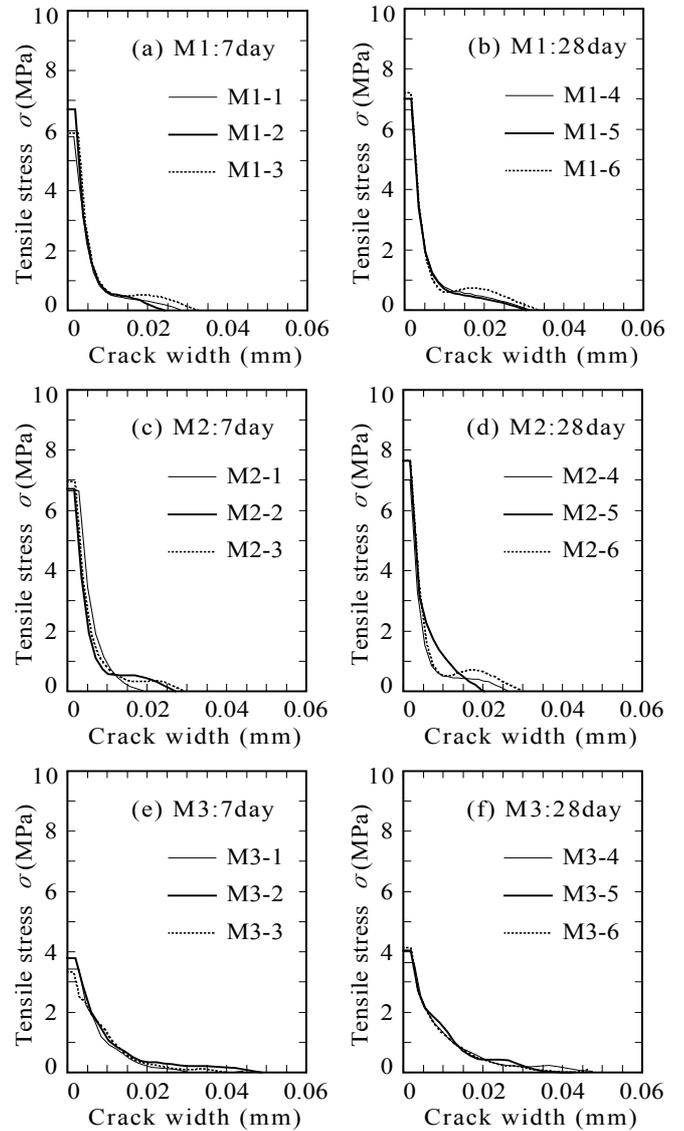Tension-softening models proposed for the concrete

Figure 6. Tension-softening diagrams determined by poly-linear inverse analysis
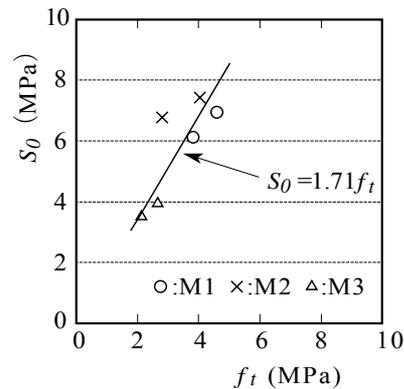

Figure 7. Relationship between calculated tensile strength S_0 and splitting tensile strength f_t

were applied to approximate the fracture behavior of mortar specimens. Figures 9 (a)~(d) show the shapes of tension-softening diagrams used for fracture analyses. Analytical results of the linear and bi-linear tension-softening models are compared to those of the

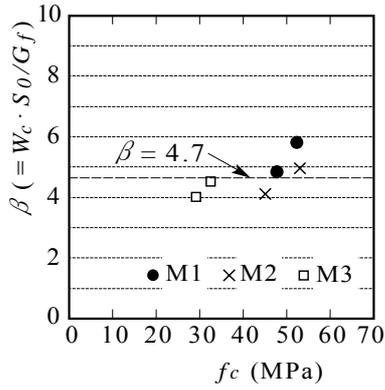hyperbolic function model proposed for the mortar.

Figure 8. Relationship between coefficient β and compressive strength f_c
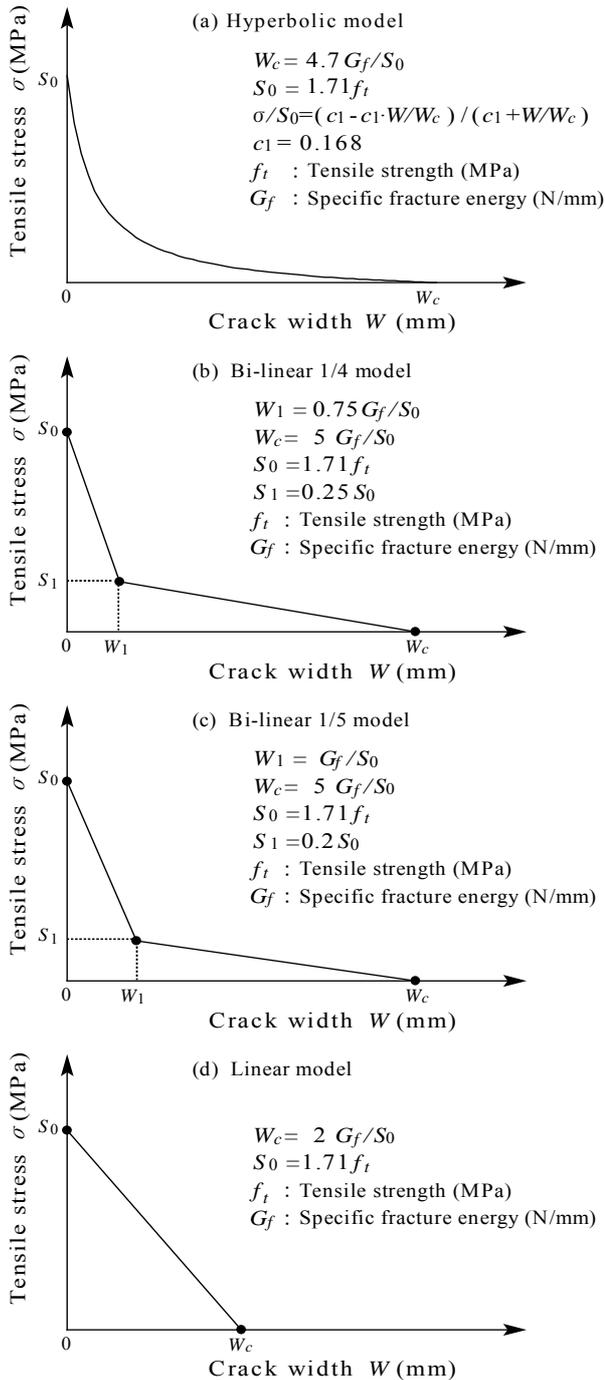

Figure 9. Tension-softening diagrams used for fracture analysis

The hyperbolic softening diagram of the mortar is calculated as follows.

$$W_c = 4.7 G_f / So \qquad (2)$$

$$\sigma / So = \frac{c_1 - c_1 \cdot W / W_c}{c_1 + W / W_c} \qquad (3)$$

where W is the crack width (mm), W_c is the critical crack width (mm), G_f is the specific fracture energy (N/mm), σ is the tensile stress, S_0 is the tensile strength (N/mm^2), S_0=1.71f_t, f_t is the splitting tensile strength (N/mm^2), c_1 is the constant (c_1=0.168).

The linear and bi-linear softening diagrams are summarized in (Kitsutaka et al. 1998) and determined by the specific values indicated in Figures 9 (b)~(d).
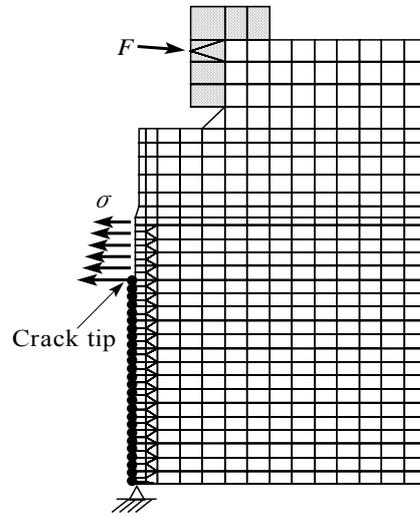

Figure 10. Finite element mesh of wedge-splitting specimen

4.2 *Simulation of wedge-splitting test*

To investigate the applicability of the tension-softening diagrams fracture analyses were carried out using the finite element method incorporated with the discrete crack model. The finite element mesh used for the analysis is shown in Figure10. The crack initiates at the notch tip and propagates along a straight line from the notch to the support. The crack tip is moved along the crack path in a step by step manner, analyzing the corresponding external loads and displacements. In every analysis stage, the stress at the crack tip is equal to the tensile strength S_0. In this analyses linear-elastic elements were used for the mortar and the material properties are given in Tables 1 and 2.

In Figures 11 (a)~(c) the load-displacement curves computed with different tension-softening diagrams are indicated for the M1, M2 and M3 mortar of 28 days. The results show that the maximum loads of the linear model are higher than those of the experiment.

The results also show that the maximum loads of the hyperbolic function model agree well with the experimental results in compared to those of the bi-linear models. Detailed comparison of the shapes and the maximum loads between the analytical and experimental results was executed, it was concluded that the results of the proposed model were accurate and close to the results of the experiment. Therefore, the tension-softening diagram based on the hyperbolic function model is reliable so that it can be used for the fracture analysis of the grouting mortar.
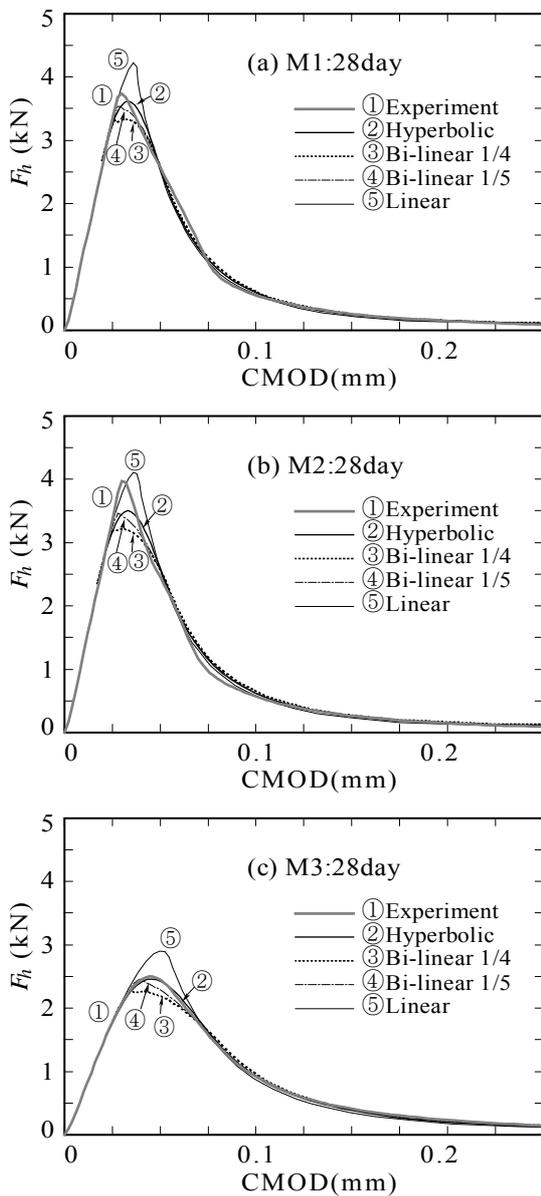

Figure 11. Load-displacement curves obtained from fracture analysis using different tension-softening diagrams

5 CONCLUSIONS

In this study the results are summarized as follows.
1. Fracture mechanical parameters of the grouting mortar were determined with the wedge-splitting and poly-linear inverse analysis method.
2. The wedge-splitting test method is appropriate to obtain a stable load-displacement curve for the grouting mortar.
3. The poly-linear inverse analysis method was useful to determine the accurate tension-softening diagrams from the wedge-splitting test results.
4. The specific fracture energy of the grouting mortar was 0.034~0.04 N/mm for the different ages of 7 and 28 days.
5. The tension-softening diagram based on the hyperbolic model was proposed and applied to the fracture analyses of mortar.
6. The experimental and analytical results indicated that the proposed model was suitable for the tension-softening diagram of the grouting mortar.

REFERENCES

Ishiguro, S. 2001. Softening properties of concrete under biaxial loading. In R.D. Borst, J. Mazars, G. P. Cabot & J. G. M. van Mier (eds.), *Proc. of the 4th Int. Conf. on Fracture Mechanics of Concrete Structures* Lisse, BALKEMA: 357-362.

Ishiguro, S., Ishii, M., Nonaka, T. & Nakagawa, H. 2004. Fracture behaviors of cementitious materials and renewed RC box culverts. In V.C. Li, C.K.Y. Leung, K. J. Willam & S. L. Billington (eds.), *Proc. of the 5th Int. Conf. on Fracture Mechanics of Concrete Structures*: 357-362.

Kitsutaka, Y., Kurihara, N. & Nakamura, N. 1998. Evaluation method of tension softening properties. In Y.Kitsutaka & H. Mihashi (eds.), *FRAMCOS-3 Pre-Conference Workshop on Quantitative Evaluation Methods for Toughness and Softening Properties of Concrete, Gifu, Japan*: 46-63.

Kitsutaka, Y., Uchida, Y., Mihashi, H., Kaneko, Y. & Nakamura, N., Kurihara, N. 2001. Draft on the JCI standard test method for determining tension softening properties of concrete. In R.D. Borst, J. Mazars, G. P. Cabot & J. G. M. van Mier (eds.), *Proc. of the 4th Int. Conf. on Fracture Mechanics of Concrete Structures* Lisse, BALKEMA: 371-376.

Mihashi, H., Kaneko, Y., Kirikoshi, K., Otsuka, K. & Akita, H. 2001. Test methods for determining tension softening diagram for concrete. In R.D. Borst, J. Mazars, G. P. Cabot & J. G. M. van Mier (eds.), *Proc. of the 4th Int. Conf. on Fracture Mechanics of Concrete Structures* Lisse, BALKEMA : 403-411.

Tschegg, E.K. 1991. New equipment for fracture tests on concrete. *Material Testing*, 33: 338-343.

Tschegg, E.K., Elser, M. & Tschegg-Stanzl, S.E. 1995. Biaxial fracture tests on concrete – development and experience. *Cement and Concrete Composites*, 17: 57-75.

Uchida, Y., Kurihara, N., Rokugo, K. & Koyanagi, W. 1995. Determination of tension softening diagrams of various kinds of concrete by means of numerical analysis. In F.H. Wittmann (ed.), *Proc. of the 2nd Int. Conf. on Fracture Mechanics of Concrete Structures,* Freiburg, Aedificatio: 17-30.